Spin waves with large decay length and few 100 nm wavelengths in thin yttrium iron garnet grown at the wafer scale

Stefan Maendl,[1, a)] Ioannis Stasinopoulos,[1] and Dirk Grundler[2, 3, b)]

[1)] *Lehrstuhl für Physik funktionaler Schichtsysteme, Physik Department E10, Technische Universität München, James-Franck-Str. 1, 85748 Garching, Germany*

[2)] *Institute of Materials (IMX) and Laboratory of Nanoscale Magnetic Materials and Magnonics (LMGN), École Polytechnique Fédérale de Lausanne (EPFL), Station 17, 1015 Lausanne, Switzerland*

[3)] *Institute of Microengineering (IMT), École Polytechnique Fédérale de Lausanne (EPFL), Station 17, 1015 Lausanne, Switzerland*

(Dated: 20 June 2017)

Using conventional coplanar waveguides (CPWs) we excited spin waves with a wavelength λ down to 310 nm in a 200 nm thin yttrium iron garnet film grown by liquid phase epitaxy. Spin-wave transmission was detected between CPWs that we separated by up to 2 mm. For magnetostatic surface spin waves we found a large nonreciprocity of 0.9 and a high group velocity v_g of up to 5.4 km/s. The extracted decay length l_d amounted to 0.86 mm. Small λ, high v_g and large l_d are key figures of merit when aiming at non-charged based signal transmission and logic devices with spin waves.

Thin films of the insulating ferrimagnet yttrium iron garnet (YIG) have recently shown to exhibit small spin-wave (SW) damping[1–7]. A large decay length of up to 0.58 mm was reported for SWs in a 20 nm thick YIG film[3]. In Ref.[3], the films were grown by pulsed laser deposition (PLD) on small substrates of (111) gadolinium gallium garnet (GGG) with a lateral size of about 10 mm × 10 mm. Small damping is important for coherent nanomagnonics, low power consumption and devices such as magnonic holography memory, non-linear cellular networks and SW interferometers[3,8–11]. Nonreciprocal characteristics of spin waves further enriches possible logic applications[12]. To scale substrate sizes up, PLD is however very challenging. Here, for instance, magnetron sputtering[13] and liquid phase epitaxy[7,14] are more suitable. Still, for decades, *commercially* available YIG films grown by liquid phase epitaxy (LPE) had a thickness of 1 μm and beyond[15]. Such thicknesses do not allow for application in nanomagnonics. Recently, a 500 nm thick LPE-grown film was explored with and without nanopatterning[16]. Parameters such as decay length l_d, group velocity v_g, and nonreciprocity parameter β were however not provided. Note that wafer bonding has already been explored to transfer LPE-grown YIG onto Si substrates to advance integrated photonics[17,18]. Such a route might be interesting for hybrid magnonic devices, and it is timely to explore in detail SW properties of thin YIG grown by LPE.

We report on experiments performed on a commercially available YIG film ordered with a thickness $t = 200$ nm that was grown by LPE on a 3" GGG substrate[20]. Using coplanar waveguides (CPWs) we explored spin-wave propagation over broad frequency and magnetic field regimes. The smallest wavelength λ that we excited by the conventional CPWs amounted to 310 nm. This value is smaller than the wavelengths so far excited via microwave antenna in thin YIG with thicknesses ranging from 20 to 500 nm[3,6,16]. At the same time, we observe modes of higher order compared to earlier publications reporting spin-wave excitation in thin YIG[3,16,21] and thin ferromagnetic metals[22,23] using bare CPWs. The nonreciprocity is found to be pronounced with a parameter β of up to 0.9, much larger compared to 20 nm thick YIG[3]. For magnetostatic surface spin waves (MSSWs) we extract a decay length of 0.86 mm that is a factor of 1.5 larger compared to Ref. [3]. The results are encouraging for prototyping nanomagnonic circuitry on large substrates with high quality
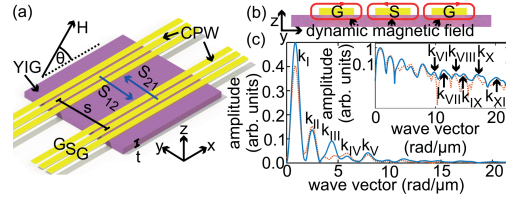
———
a)stefan.maendl@ph.tum.de
b)dirk.grundler@epfl.ch

FIG. 1. (a) YIG of thickness t investigated by coplanar waveguides (CPWs). The separation s ranged from 60 μm to 2 mm. (b) Sketch of the dynamic magnetic field $\mathbf{h}$ (lines with arrows around ground (G) and signal (S) lines). (c) Excitation strength as a function of wave vector k for a CPW with $w = 2.1$ μm and $r = 1.2$ μm. The full (dotted) line represents the Fourier analysis of component $h_z(y)$ [$h_y(y)$] of $\mathbf{h}$. The inset contains the simulated data in a half-logarithmic graph. Labels indicate relevant peaks.
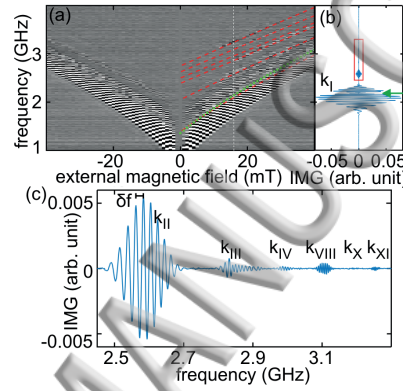

FIG. 2. (a) Imaginary (IMG) part of ΔS_{12} obtained in MSSW configuration (white - positive values, black - negative values). The slanted broken lines indicate eigenfrequencies calculated for different fixed k[19]. (b) Line plot ΔS_{12} taken at 16 mT [white dashed line in (a)]. The arrow indicates a node that we attribute to an anticrossing between a MSSW and PSSW. (c) Enlarged signal from the rectangular box shown in (b). Oscillations indicate propagating spin waves. Labels refer to different wave vectors (Tab. I).

thin YIG that supports nonreciprocal spin waves.

From the 3" wafer, we cut samples with different lateral sizes of about 6×6 mm^2 and 2×8 mm^2. To excite spin-processional motion we integrated CPWs[24,25] [Fig. 1 (a) and (b)], consisting of a 4.5 nm thick chromium and 120 nm thick gold layer. We connected a multi-port vector network analyzer (VNA) to measure scattering parameters S_{12} and S_{21} between two neighboring CPWs [Fig. 1 (a)]. We explored different separations s ranging from 60 μm to 2 mm. For small s, the width w of ground (G) and signal (S) lines amounted to 2.1 ± 0.2 μm. Their length l was 380 μm. The edge-to-edge separation (gap) r between G and S was 1.2 ± 0.2 μm. The characteristic excitation strength of the CPWs was obtained from simulations of its magnetic field $\mathbf{h}$[26]. The Fourier analysis is displayed in Fig. 1 (c) as a function of wave vector k that is transferred to spin waves in YIG. The in-plane $\mathbf{k}$ was perpendicular to the signal line. For large s, we used CPWs with the following parameters: $w = 3$ μm, $r = 2$ μm, $l = 2$ mm. The VNA output power amounted to -20 dBm, if not stated otherwise. The external magnetic field $\mathbf{H}$ was applied in the sample plane in different orientations indicated by the angle θ. We used the imaginary part (magnitude) of scattering parameters S to extract v_{g} (nonreciprocity β). To remove field-independent background signals originating from the setup we subtracted a reference spectrum taken at 0 mT obtaining spectra ΔS. The damping constant of $\alpha = 1.0 \cdot 10^{-4}$, saturation magnetization $M_{\mathrm{s}} = 140$ kA/m, and exchange constant $A = 0.332 \times 10^{-6}$ erg/cm were extracted from a sample that was positioned on a 20 μm wide CPW in flip-chip configuration and investigated in a perpendicular field H. Values were consistent with Refs. [2, 27–29]. From α we

label	k (rad/μm)	λ (μm)	v_{g} (km/s)	label	k (rad/μm)	λ (μm)	v_{g} (km/s)
k_{I}	0.9	6.98	2.58	k_{VIII}	13.5	0.47	0.30
k_{II}	2.5	2.51	1.32	k_{X}	16.9	0.37	0.30
k_{III}	4.5	1.40	0.66	k_{XI}	20.0	0.31	0.24
k_{IV}	5.9	1.06	0.48				

TABLE I. Spin-wave wave vectors k, corresponding wavelengths $\lambda = 2\pi/k$ and group velocities v_{g} extracted from Fig. 2 at 16 mT.

calculated the relaxation time τ considering[30]

$$\tau = \frac{1}{2\pi\alpha f} \tag{1}$$

and an ellipticity factor of one[31]. Here, f is the resonance frequency at $k = 0$. Our value of $\alpha = 1.0 \times 10^{-4}$ was similar to the value of $\alpha = 1.2 \times 10^{-4}$ reported very recently for a 106 nm thick YIG film grown by LPE[7]. It is larger compared to PLD-grown and sputtered YIG that was reported to exhibit $\alpha \leq 1 \times 10^{-4}$ [5,13]. To calculate spin-wave dispersion relations $f(\mathbf{k}, \mathbf{H})$ we applied the formalism of Kalinikos and Slavin[19] with parameters given above and gyromagnetic splitting factor $\gamma = 2.83$ MHz/Oe[13].

In Fig. 2 (a) gray-color-coded spectra ΔS_{12} are shown taken with different H parallel to the CPW. The graph shows the imaginary part of S_{12}. At large H, the magnetization $\mathbf{M}$ is perpendicular to $\mathbf{k}$ and we encounter the magnetostatic spin-wave (MSSW) configuration. The black-white oscillating contrast is consistent with spin waves propagating between CPW1 and CPW2.[32] For positive H, up to seven different modes are resolved [compare lineplots extracted for 16 mT and shown in Fig. 2 (b) and (c)]. The formalism of Ref. [19] allowed us to model the field dependencies of eigenfrequencies [dashed lines in Fig. 2 (a)] and thereby identify the wave vectors k of propagating spin waves as highlighted by the labels in Fig. 2 (b) and (c) and listed in Tab. I. For negative H, less modes were resolved due to nonreciprocity that will be discussed below. In the spectra [Fig. 2 (b)] we identified a specific node (arrow) in the signal labelled by k_{I}. The node indicated that propagation between CPW1 and 2 was suppressed at a specific frequency. We attribute the suppression to an anticrossing between the mode with $\mathbf{M} \perp \mathbf{k}$ (Damon-Eshbach mode) and the Perpendicular Standing Spin Wave (PSSW) of first order[33]. The calculated eigenfrequency of the PSSW[19] is shown as a dotted line in Fig. 2 (a). The line reproduces well the field dependence of the node, i.e., the signal suppression. This is because the PSSW is almost independent of the in-plane wave vector k for small k. Its eigenfrequency thus reflects well the center frequency of the gap induced by the anticrossing.

We now extract group velocities v_{g} of propagating SWs from the oscillating contrast shown in Fig. 2 (a). The group velocity is calculated by $v_{\mathrm{g}} = \delta f \cdot s$, where δf is the frequency separation between neighboring local maxima (or minima) in S_{12} [Fig. 2 (c)]. In Fig. 3 (a) we summarize the values v_{g} (symbols) as a function of H that we extract from the most intensive signal reflecting wave vectors k_{I} [Fig. 1 (c)]. The group velocity amounts to 5.4 km/s at 1 mT. For fixed k, it decreases continuously with H as commonly observed[34,35]. The value of 5.4 km/s is four times larger than the value reported by Yu et al.[3] for 20 nm thin YIG. The larger thickness t used here increases dipolar forces and enhances the slope $v_{\mathrm{g}} = 2\pi df/dk$ of $f(k)$ at small k. Similarly large values have been reported for 82 nm thick YIG grown by PLD for which, however, the modelling needed to consider a growth-induced magnetic anisotropy[35].

In Fig. 3 (b) we show the dependence of v_{g} (symbols) on wave vector k for fixed field $\mu_0 H = 16$ mT where we resolved seven modes discussed above. A maximum group velocity of 2.6 km/s is measured for k_{I}. For larger k, v_{g} first decreases and then seems to level off. Corresponding values are listed in Tab. I. The lines in Fig. 3 (a) and (b) represent calculated dependencies[19]. We find a good quantitative agreement between experiment and theory for $\mu_0|H| \geq 5$ mT. The dispersion relation $f(k)$ at 16 mT is shown as a line in Fig. 3 (c). The
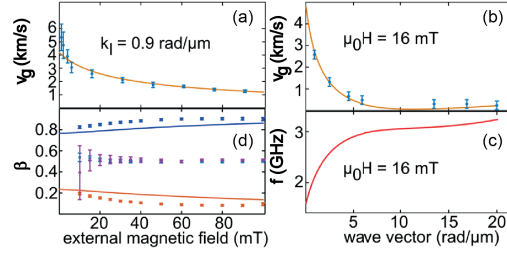
FIG. 3. (a) Group velocity dependent on H as measured in the MSSW configuration for $k = k_I$ (symbols). (b) Group velocities as a function of k and (c) dispersion relation $f(k)$ at 16 mT. The experimental values are extracted from spectra shown in Fig. 2 (a) to (c). The lines in (a) to (c) are calculated using the formalism of Ref.[19]. (d) Nonreciprocity parameter β of spin waves with wave vector k_I in MSSW (top and bottom most symbols) and BVMSW configuration (central symbols). The top most (bottom most) symbols reflect S_{12} (S_{21}) taken at $H > 0$. The lines depict the calculated nonreciprocity in MSSW configuration.

shape of $f(k)$ highlights that our experiments addressed both dipolar (magnetostatic) and dipole-exchange spin waves in the thin YIG[36]. For 7 rad/μm $< k <$ 12 rad/μm, $f(k)$ is almost constant and $v_g = 2\pi df/dk$ is predicted to be (vanishingly) small. In the spectrum of Fig. 1 (c) we do not resolve propagation signals for wave vectors k_V, k_{VI}, k_{VII} and k_{IX} provided by the CPW. These values fall in the wave vector regime where the calculated SW dispersion relation is flat and v_g approaches zero. Correspondingly, propagation is expected to be weak consistent with the experimental observation. Still we resolve k_{VIII}. We attribute this to the fact that for k_{VIII} both components h_x and h_z have a local maximum in Fig. 1 (c). Here, the combined torque acting on the spins might induce an appreciable spin-wave amplitude that still reaches the detector despite the small v_g.

In Fig. 3 (d) we depict the nonreciprocal characteristics of the k_I excitation for both the MSSW ($\theta = 0$ deg) and Backward Volume Magnetostatic Spin Wave (BVMSW) configuration ($\theta = 90$ deg). We summarize the maximum amplitude a' of the linear magnitude of ΔS_{12} and ΔS_{21} at different H. We extract the nonreciprocity using

$$\beta = \frac{a'(S_{12}(H))}{a'(S_{12}(-H)) + a'(S_{12}(H))}. \tag{2}$$

For BVMSW modes, we find β close to 0.5, i.e., reciprocal behavior consistent with Ref. [37]. For the MSSW mode we obtain a large nonreciprocity β of up to 0.9 (0.1) for S_{12} (S_{21}) at large H of 100 mT. β extracted from S_{12} is found to decrease when reducing H. This behavior has been reported for ferromagnetic metals as well[12]. The field dependence of β for the MSSW mode is consistent with the behavior [solid lines in Fig. 3 (d)] calculated from the intrinsic nonreciprocity of the MSSW surface wave[38] combined with the direction-dependent excitation characteristics of our antenna[39] (see Eqs. (S1) to (S5)). The observed characteristics is advantageous for nonreciprocity-based magnonic devices[12].

To investigate the decay length l_d of propagating spin waves we mounted a YIG sample face-down on two different sets of 2 mm long CPWs. The sample was 2 mm wide and about 8 mm long. Both ends were cut at 45 deg to avoid reflections. The k_I excitation of the CPWs was calculated to be at 0.4 rad/μm[26]. The signal ΔS_{12} measured for a distance $s = 2$ mm between two neighboring CPWs is shown in Fig. 4. The distance s is larger by a factor of 28.5 compared to Ref.[40]. The spectrum ΔS_{12} taken at -20 mT features an oscillating signal indicating propagating spin waves (inset). The signal ΔS_{12} measured for CPWs with a smaller s of 1 mm (not shown) was larger by a factor of 2.5. In Fig. 4 (b) we compare the measured signal strengths for different s. The data point at $s = 0$ represents the signal strength expected when considering the nonreciprocity in the given MSSW configuration. The straight line indicates a decay length of $l_d = 0.86 \pm 0.05$ mm.

We now calculate the decay length $l_d = v_g \cdot \tau$ from the Gilbert damping parameter of $\alpha = 1.0 \cdot 10^{-4}$ that we extracted in perpendicular magnetic fields by which two-magnon scattering was suppressed[41]. Assuming the relevant FMR frequency $f = 1.78$ GHz at 20 mT
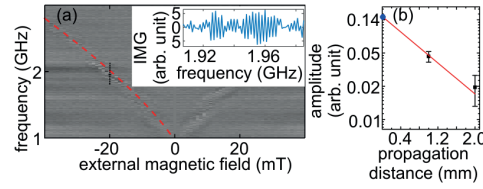
This manuscript was accepted by Appl. Phys. Lett. Click here to see the version of record.

5

FIG. 4. (a) Color-coded spectra ΔS_{12} obtained on the YIG film by two parallel CPWs separated by 2 mm (flip-chip geometry). H was applied parallel to the CPWs. The inset displays the imaginary (IMG) part of ΔS_{12} at -20 mT (vertical broken line). The dashed line represents calculated eigenfrequencies for $k = k_I$[19]. (b) Amplitudes measured in ΔS_{12} for k_I and normalized to ΔS_{22} at -20 mT for two different s. The power at the VNA was -10 dBm. At $s = 0$ we depict the normalized signal strength considering the nonreciprocity parameter $\beta = 0.15$ for the given MSSW configuration. The solid line reflects a decay length of 0.86 mm.

in Eq. (1) and $v_g = 2.5$ km/s, we calculate $l_d = 2.2$ mm. This value is a factor of 2.6 larger than the measured one. We attribute the discrepancy to the scattering of propagating magnons at both defects in YIG and the regions where CPW ground lines modify $f(k)$[3,40]. Furthermore an unintentional amplitude variation might have occurred in the different data points of Fig. 4 (b) if a dust particle had varied the separation between sample and CPWs in the flip-chip geometry used. Considering these aspects, the decay length of 0.86 mm extracted experimentally for the LPE-grown YIG film reflects a reasonable value.

We now discuss recently published values for decay lengths $l_d = v_g\tau$ in thin YIG grown on small substrates by PLD. For a given damping parameter α, τ is large for small f of a MSSW [Eq. (1)]. The same holds true for v_g[34]. At a frequency of 1.1 GHz and a group velocity $v_g = 1.16$ km/s a decay length of 0.58 mm was reported for 20 nm thick YIG in an in-plane field of 5 mT[3]. Here the damping parameter α amounted to $2.3 \cdot 10^{-4}$. For a microstructured waveguide prepared from 20 nm thick YIG a consistently smaller decay length of 0.025 mm was found at 45 mT with $v_g = 0.35$ km/s, $\alpha = 4\cdot10^{-4}$ and $f = 3$ GHz[40]. Note that for a given thin film, l_d in general decreases with increasing field (or increasing frequency) and decreasing waveguide width in the dipolar regime of the MSSW. In Ref.[42], 40 nm thick YIG with $\alpha = 3.1 \cdot 10^{-4}$ was prepared by magnetron sputtering. Here, at 6 GHz and 130 mT an edge mode was reported to transmit spin-wave signals up to 0.15 mm. The values of Refs.[3,40,42] all outperform the scattering length (mean free path) of electrons (which is typically on the order of 0.0001 mm) and enable coherent processing of information in a mesoscopic network. However, larger decay lengths l_d are still advantageous to minimize the loss of magnonic devices.

In the long wavelength limit, small frequencies near 1 GHz are typically needed to guarantee for a large v_g and large l_d[3,35]. Exchange-dominated spin waves with wavelengths smaller than 100 nm can exhibit large v_g in thin YIG as well[43]. Here, f is around 10 GHz or even larger. In Ref.[43] spin waves with $\lambda = 88$ nm were excited in thin YIG using grating couplers underneath CPWs. The measured group velocity amounted to 1.2 km/s at 90 mT. Note that v_g increases with increasing k in the exchange-dominated regime. Further optimized microwave-to-magnon transducers based on e.g. grating couplers[43], individual nanomagnets[44], or sample edges[45] will allow one to excite spin waves with small λ and relatively large v_g in the exchange-dominated regime. Still, related decay lengths need to be explored.

In conclusion we showed that 200 nm thick YIG grown by liquid phase epitaxy supported spin waves with a group velocity of up to 5.4 km/s, a large nonreciprocity of $\beta = 0.9$ and small wavelengths down to 310 nm when excited by a conventional CPW. The large β was attributed to the nonreciprocity of the excited surface wave combined with the direction-dependent excitation characteristics of the microwave antenna. At a frequency of about 2 GHz we observed spin-wave propagation over 2 mm between two coplanar waveguides. Importantly, LPE allows one to deposit thin epitaxial YIG of high quality on large-area GGG substrates and is hence complementary to magnetron sputtering that already provided extremely low damping parameters. Long decay lengths are a prerequisite when aiming at

coherent information processing in integrated nanomagnonic networks at low power consumption.
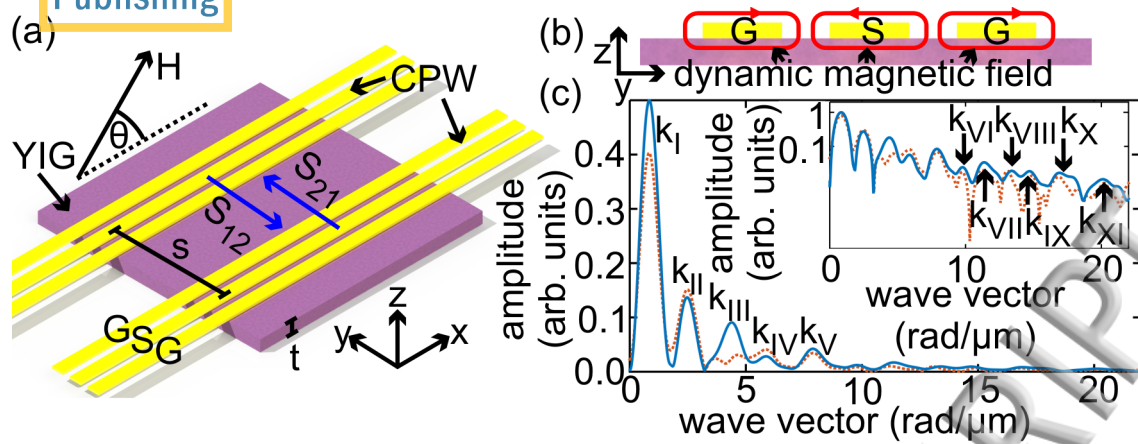
SUPPLEMENTARY MATERIAL

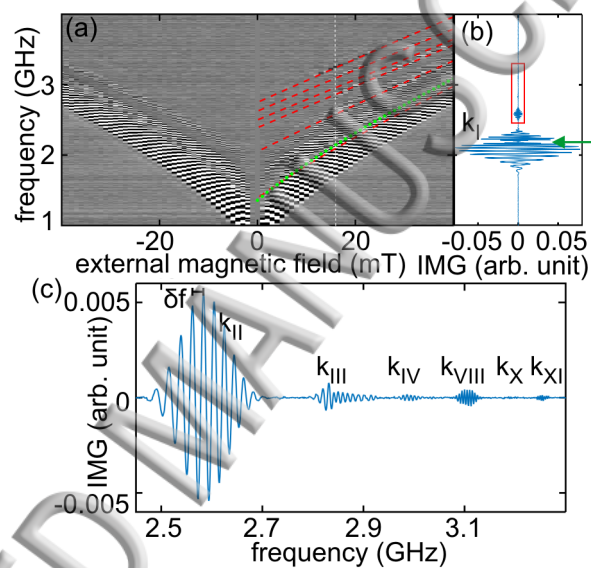See supplementary material for calculation of nonreciprocity.
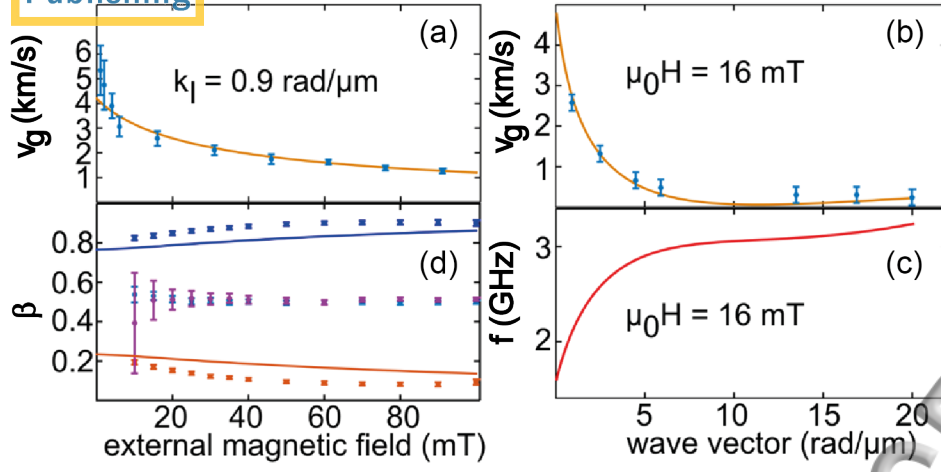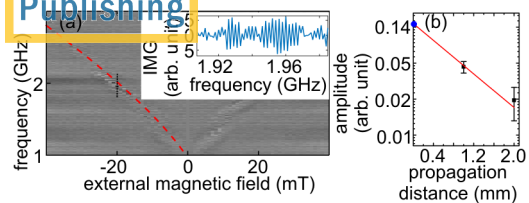
ACKNOWLEDGMENT

[1] B. Heinrich, C. Burrowes, E. Montoya, B. Kardasz, E. Girt, Y.-Y. Song, Y. Sun, and M. Wu, Phys. Rev. Lett. **107**, 066604 (2011).

[2] O. d'Allivy Kelly, A. Anane, R. Bernard, J. B. Youssef, C. Hahn, A. H. Molpeceres, C. Carrétéro, E. Jacquet, C. Deranlot, P. Bortolotti, *et al.*, Appl. Phys. Lett. **103**, 082408 (2013).

[3] H. Yu, O. d'Allivy Kelly, V. Cros, R. Bernard, P. Bortolotti, A. Anane, F. Brandl, R. Huber, I. Stasinopoulos, and D. Grundler, Sci. Rep. **4**, 6848 (2014).

[4] M. B. Jungfleisch, W. Zhang, W. Jiang, H. Chang, J. Sklenar, S. M. Wu, J. E. Pearson, A. Bhattacharya, J. B. Ketterson, M. Wu, and A. Hoffmann, J. Appl. Phys. **117**, 17D128 (2015), http://dx.doi.org/10.1063/1.4916027.

[5] C. Hauser, T. Richter, N. Homonnay, C. Eisenschmidt, M. Qaid, H. Deniz, D. Hesse, M. Sawicki, S. G. Ebbinghaus, and G. Schmidt, Sci. Rep. **6**, 20827 (2016).

[6] L. V. Lutsev, A. M. Korovin, V. E. Bursian, S. V. Gastev, V. V. Fedorov, S. M. Suturin, and N. S. Sokolov, Appl. Phys. Lett. **108**, 182402 (2016).

[7] C. Dubs, O. Surzhenko, R. Linke, A. Danilewsky, U. Brückner, and J. Dellith, J. Phys. D: Appl. Phys. **50**, 204005 (2017).

[8] A. V. Chumak, V. I. Vasyuchka, A. A. Serga, and B. Hillebrands, Nat. Phys. **11**, 453 (2015).

[9] A. Khitun, M. Bao, and K. L. Wang, J. Phys. D: Appl. Phys. **43**, 264005 (2010).

[10] M. M. Eshaghian-Wilner, A. Khitun, and K. L. Wang, US Patent **8,193,598**, B2 (2012).

[11] F. Gertz, A. Kozhevnikov, Y. Filimonov, and A. Khitun, IEEE Tran. Magn. **51**, 1 (2015).

[12] M. Jamali, J. H. Kwon, S.-M. Seo, K.-J. Lee, and H. Yang, Sci. Rep. **3**, 3160 (2013).

[13] H. Chang, P. Li, W. Zhang, T. Liu, A. Hoffmann, L. Deng, and M. Wu, IEEE Magn. Lett. **5**, 6700104 (2014).

[14] V. Castel, N. Vlietstra, B. van Wees, and J. B. Youssef, Phys. Rev. B **86**, 134419 (2012).

[15] A. Serga, A. Chumak, and B. Hillebrands, J. Phys. D: Appl. Phys. **43**, 264002 (2010).

[16] Y. Khivintsev, Y. Filimonov, and S. Nikitov, Appl. Phys. Lett. **106**, 052407 (2015).

[17] M.-C. Tien, T. Mizumoto, P. Pintus, H. Kromer, and J. E. Bowers, Opt. Express **19**, 11740 (2011).

[18] D. Huang, P. Pintus, C. Zhang, P. Morton, Y. Shoji, T. Mizumoto, and J. E. Bowers, Optica **4**, 23 (2017).

[19] B. A. Kalinikos and A. N. Slavin, J. Phys. C: Sol. St. Phys. **19**, 7013 (1986).

[20] Matesy GmbH, Otto-Schott-Str. 13, 07745 Jena, Germany.

[21] J. Chen, F. Heimbach, T. Liu, H. Yu, C. Liu, H. Chang, T. Stckler, J. Hu, L. Zeng, Y. Zhang, Z. Liao, D. Yu, W. Zhao, and M. Wu, J. Magn. Magn. Mat. , (2017).

[22] V. Vlaminck and M. Bailleul, Phys. Rev. B **81**, 014425 (2010).

[23] F. Ciubotaru, T. Devolder, M. Manfrini, C. Adelmann, and I. P. Radu, Appl. Phys. Lett. **109**, 012403 (2016), http://dx.doi.org/10.1063/1.4955030.

[24] G. Counil, J.-V. Kim, T. Devolder, C. Chappert, K. Shigeto, and Y. Otani, J. Appl. Phys. **95**, 5646 (2004).

[25] S. Neusser, G. Duerr, H. Bauer, S. Tacchi, M. Madami, G. Woltersdorf, G. Gubbiotti, C. Back, and D. Grundler, Phys. Rev. Lett. **105**, 067208 (2010).

[26] *CST Microwave Studio 2014, CST Computer Simulation Technology, www.cst.com*.

[27] J. E. Kunzler, L. R. Walker, and J. K. Galt, Phys. Rev. **119**, 1609 (1960).

[28] D. T. Edmonds and R. G. Petersen, Phys. Rev. Lett. **2**, 499 (1959).

[29] S. Klingler, A. Chumak, T. Mewes, B. Khodadadi, C. Mewes, C. Dubs, O. Surzhenko, B. Hillebrands, and A. Conca, J. Phys. D: Appl. Phys. **48**, 015001 (2015).

[30] D. D. Stancil, *Theory of magnetostatic waves* (Springer, New York, 1993).

[31] V. Kambersky and C. Patton, Phys. Rev. B **11**, 2668 (1975).

[32] M. Bailleul, D. Olligs, and C. Fermon, Appl. Phys. Lett. **83**, 972 (2003).

[33] P. Grünberg, in *Light Scattering in Solids V* (Springer, 1989) pp. 303–335.

[34] H. Yu, R. Huber, T. Schwarze, F. Brandl, T. Rapp, P. Berberich, G. Duerr, and D. Grundler, Appl. Phys. Lett. **100**, 262412 (2012).

[35] A. Krysztofik, H. Gowiski, P. Kuswik, S. Zitek, E. Coy, J. Rychy, S. Jurga, T. Stobiecki, and J. Dubowik, J. Phys. D: Appl. Phys. (2017).

[36] A. G. Gurevich and G. A. Melkov, *Magnetization Oscillations and Waves* (CRC Press, 1996).

[37] A. V. Chumak, V. S. Tiberkevich, A. D. Karenowska, A. A. Serga, J. F. Gregg, A. N. Slavin, and B. Hillebrands, Nat. Comm. **1**, 141 (2010).

[38] G. Melkov, V. Vasyuchka, A. Chumak, V. Tiberkevich, and A. Slavin, J. Appl. Phys. **99**, 08P513 (2006).

[39] V. E. Demidov, M. P. Kostylev, K. Rott, P. Krzysteczko, G. Reiss, and S. O. Demokritov, Appl. Phys. Lett. **95**, 112509 (2009).

[40] M. Collet, O. Gladii, M. Evelt, V. Bessonov, L. Soumah, P. Bortolotti, S. O. Demokritov, Y. Henry, V. Cros, M. Bailleul, V. E. Demidov, and A. Anane, Appl. Phys. Lett. **110**, 092408 (2017), http://dx.doi.org/10.1063/1.4976708.

[41] R. Arias and D. L. Mills, Phys. Rev. B **60**, 7395 (1999).

[42] A. Talalaevskij, M. Decker, J. Stigloher, A. Mitra, H. S. Körner, O. Cespedes, C. H. Back, and B. J. Hickey, Phys. Rev. B **95**, 064409 (2017).

[43] H. Yu, O. d'Allivy Kelly, V. Cros, R. Bernard, P. Bortolotti, A. Anane, F. Brandl, F. Heimbach, and D. Grundler, Nat. Commun. **7**, 11255 (2016).

[44] Y. Au, E. Ahmad, O. Dmytriiev, M. Dvornik, T. Davison, and V. V. Kruglyak, Appl. Phys. Lett. **100**, 182404 (2012), http://dx.doi.org/10.1063/1.4711039.

[45] C. S. Davies and V. V. Kruglyak, IEEE Trans. Magn. **52**, 2300504 (2016).

(a)

(b)

(c)

(a)

(b)